

TENSILE HYDRAULIC FRACTURE OF CONCRETE AND ROCK

J.H.M. Visser and J.G.M. van Mier,
Stevin Laboratory II, Department of Civil Engineering, Delft University of
Technology, Delft, The Netherlands

Abstract

Tensile failure envelopes have been obtained from triaxial hydraulic fracture experiments on a mortar and a sandstone. Both materials have been tested unsaturated and water saturated. Only the saturated sandstone specimens have been tested with free fluid penetration from the reservoir of the triaxial cell. For the other three test series, fluid penetration was prohibited. The failure envelopes for the four tested situations are approximated by linear functions of the radial and axial failure stresses. Tensile failure of the unsaturated materials in closed conditions depends on both the radial and the axial stress, although the contribution of the radial stress to the tensile failure differs for the two materials. Tensile failure of fluid saturated materials is influenced by the hydrostatic pore pressure, which reduces the effect of the radial compressive stress on the material. Nevertheless, the contribution of the radial stress can not be excluded. An effective axial stress law will therefore not adequately predict tensile failure of the tested materials. Other failure criteria still have to be investigated.

1 Introduction

Hydraulic fracturing of concrete and rock is the fracturing of the material under a fluid pressure. The fluid pressure can be imposed externally (e.g. water pressure on a dam) or internally (i.e. pore fluid pressure). A tensile fracture will be initiated hydraulically when the net fluid pressure exceeds the tensile strength of the material. Once a fracture is initiated, the fracture may get fluid-filled, either by communication of the fracture with the external fluid or by pore fluid drainage from the material. The pressurized fluid in the fracture will impose an extra body force on the fracture faces and may serve as the main driving force for fracture propagation. When the material is permeable, the state of stress will be changed by fluid flows (e.g. from the fracture in the material), thereby influencing the hydraulic fracture process. The hydraulic fracture problem is thus a highly coupled problem between pore fluid, fracture fluid and solid material. At the moment, however, the coupling mechanisms are barely understood.

In order to investigate the coupling effects in fluid saturated materials, hydraulic fracture experiments in tension have been carried out with a triaxial cell. In this paper, the experimental set-up will be described briefly. Results will be shown, with respect to the fracture initiation stresses. Interpretation of the results will focus on the failure mechanisms at the particle level.

2 Experiments

2.1 Experimental set-up

The hydraulic fracture experiments are performed with a triaxial cell, which has been designed for deformation controlled experiments in the tensile regime. A cross sectional view of the cell is given in Fig. 1. For a detailed description of the triaxial cell and the regulation system, see Visser and Van Mier, 1992. In the triaxial cell, cylindrical specimens are loaded in the radial direction by pressurizing the fluid in the reservoir of the cell and in the axial direction by a hydraulic actuator. In the axial direction, both a tensile and a compressive load can be applied. The applied load paths are such that the specimens always fails in tension, with the fracturing plane perpendicular to the axis of the cylinder. Two different load paths are used (see Fig. 2). For both load paths, the specimen is loaded first to a certain hydrostatic stress. For load path 1, the radial pressure is then kept constant while the axial compressive load is slowly reduced. For load path 2 the axial compressive load is kept constant after

hydrostatic loading while the radial fluid pressure is increased. For both load paths, the experiments are performed in axial deformation control.

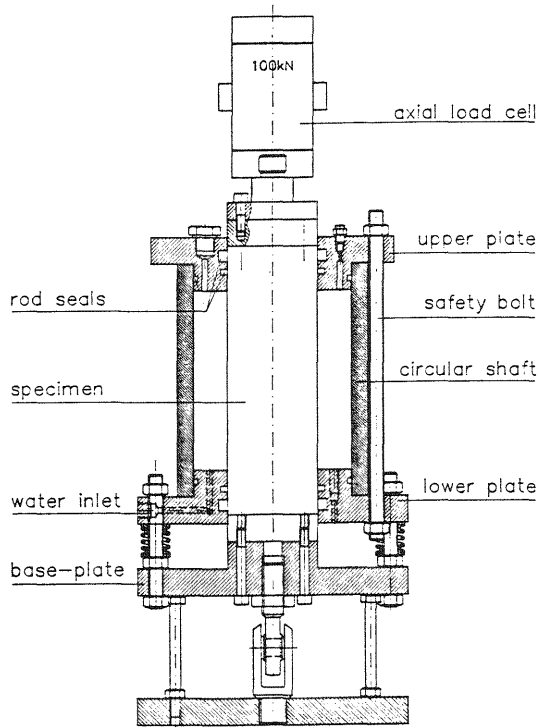


Fig. 1 The hydraulic cell

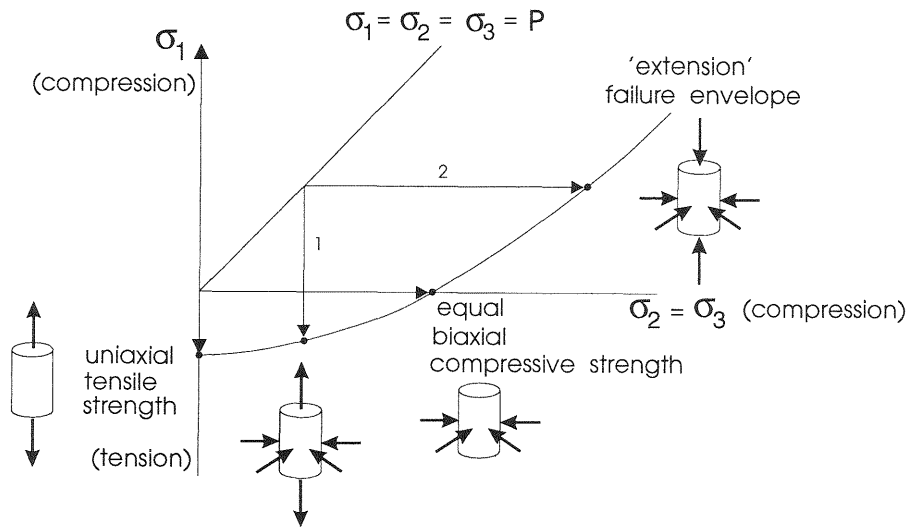


Fig. 2 Load paths investigated

2.2 Specimens.

Three types of cylindrical specimens have been used in the experiments. Geometry and dimensions of the specimens are shown in Fig. 3. The specimen length is dictated by the boundary conditions (see Visser, 1995). Furthermore, all specimens have a circular notch, to define the region of fracturing. Four LVDTs are attached to the specimen at a 90 degrees interval and placed over the notch in longitudinal direction by holders glued to the specimens surface. The manufacturing and the specifications of the specimens are given in Visser (1995).

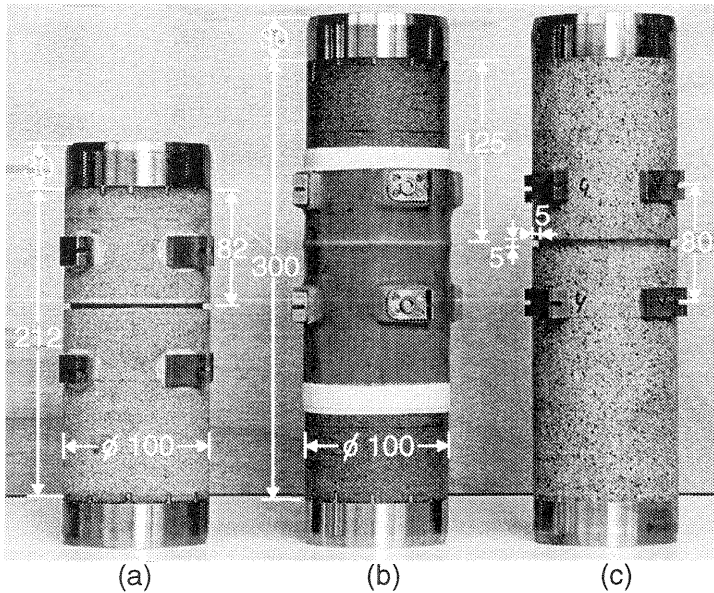


Fig. 3 Dimensions of an open sandstone specimen (a), a closed sandstone specimen (b) and a mortar specimen (c)

2.3 Performed experiments.

In this paper, the results of four test series are presented. The results of the first two series are obtained from experiments on mortar specimens under closed conditions (i.e. without fluid penetration from the reservoir of the cell). Closed conditions have been achieved by using a viscous oil for which the mortar is impermeable. The oil is allowed to enter the fracture once initiated. The mortar specimens have been tested unsaturated and water saturated. In the third and fourth series, Felsler sandstone specimens have been tested. The third series has been performed on unsaturated sandstone under closed conditions. Closed conditions for the sandstone are achieved by using a sleeve since the sandstone is highly permeable to all fluids (see Fig. 3b). An additional effect of the sleeve is that the reservoir fluid can not enter the fracture once initiated. In the fourth series, water

saturated sandstone has been tested under the condition of free fluid flow. This means that there is free communication between reservoir, fracture and pore fluid. In both sandstone series, water was used as a reservoir fluid.

3 Results

As illustrative examples of the results, response curves of saturated mortar specimens at different constant radial compressive stresses are given in Fig. 4. The axial stress and elongation are given relative to the hydrostatic pre-loading values (compression=positive). The response curves are typical for heterogeneous materials like the mortar and the sandstone. The unsaturated mortar and sandstone specimens show a similar response.

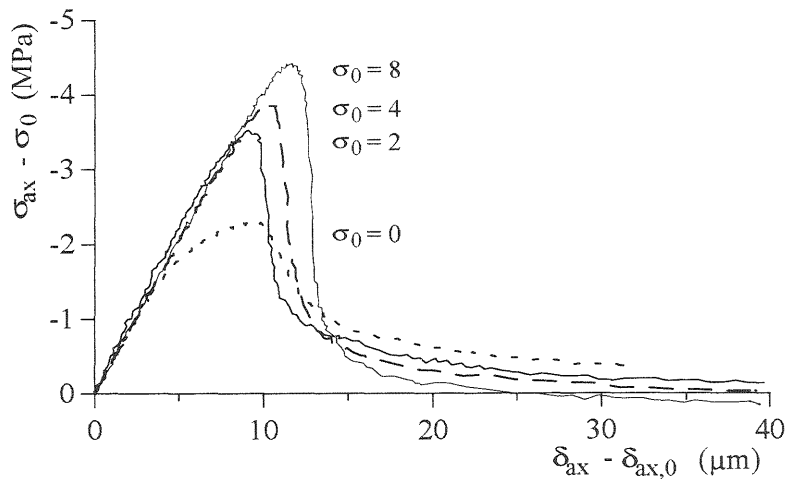


Fig. 4 Response curves of the saturated mortar specimens for different hydrostatic pre-loading stresses

From the response curves of the experiments of the four series, peak stresses were interpreted as the failure stresses of the material. It is assumed that at the failure stress, a major fracture is initiated. The failure stresses for the mortar specimens are given in Fig. 5 and for the sandstone specimens in Fig. 6.

4 Interpretation of the results

4.1 Uniaxial tensile strength

The uniaxial tensile strength of the material is defined as the maximum

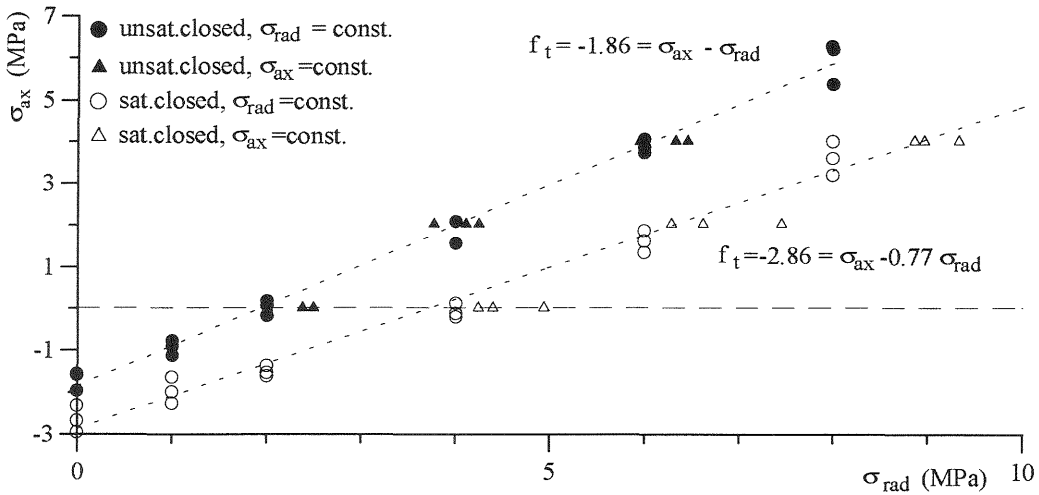


Fig. 5 Failure stresses for the mortar specimens

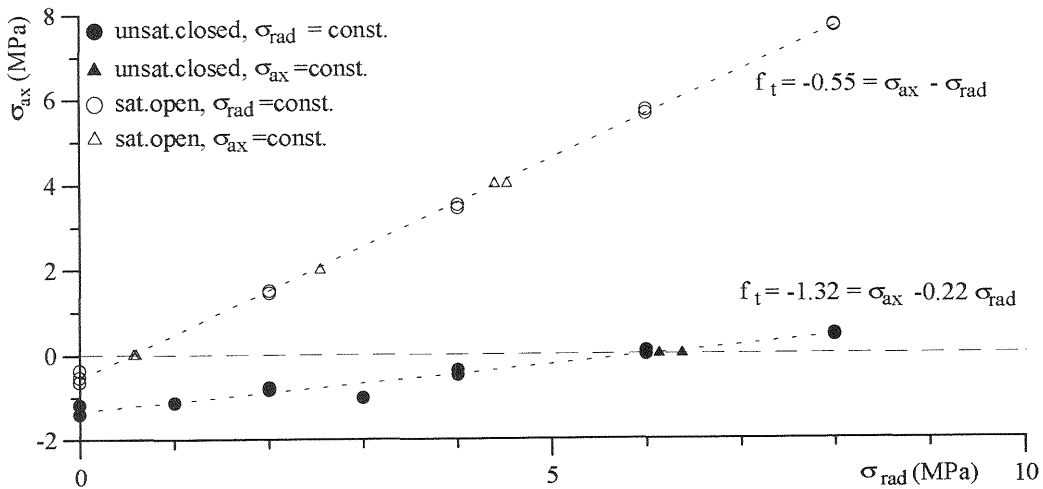


Fig. 6 Failure stresses for the Felsler sandstone specimens

tensile stress the material can sustain. Hence, it is equal to the uniaxial tensile failure stress of the material. The uniaxial tensile strength is determined by the meso-mechanical behaviour of the material. At this level, the tested materials consist of aggregates embedded in a porous matrix. Under a global uniaxial tensile load, both local compressive and tensile stresses exist in the material. At the meso-level different failure modes are possible, but tensile microcracking of the bond between the aggregates and matrix will dominate due to the relatively low tensile strength of the bonds (Mindess, 1989). This is indicated in Fig. 7a, where the material is depicted by four aggregates in the matrix, with a pore in between the aggregates. The tensile strength can thus be expected to

depend strongly on the tensile bond strength between aggregates and matrix. In addition to the bond strength, the tensile strength of the materials depends on the transmission of the load through the material. Number of bonds and bond direction, for instance, will influence the local tensile stress at the bond. Furthermore the strength is also determined by the ease with which bond cracks are able to align to a major fracture. Alignment of the microcracks depends, among others, on the composition and distribution of the constituents, the strength (ratios) of the internal and coupling bonds and porosity. For example, if the distribution of the aggregates is sparse, alignment can be obtained only by continued cracking of the matrix material, while for a dense aggregate distribution, continued bond cracking may suffice for alignment. The latter case will occur at a lower stress due to the low strength of the matrix-aggregate bond.

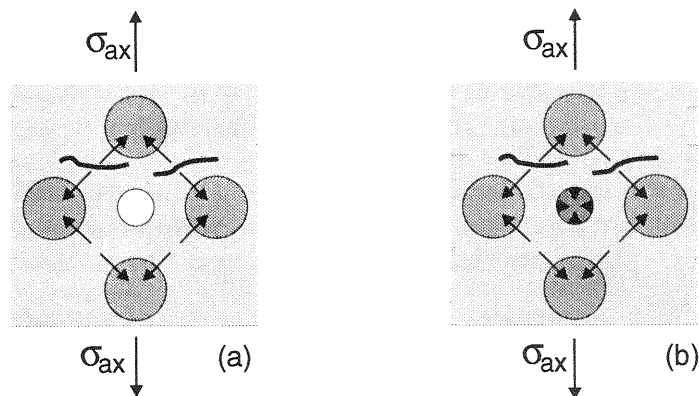


Fig. 7 Reaction forces under a global tensile stress for an unsaturated (a) and a saturated (b) porous material

From the above discussion, it is clear that the tensile strength depends on the mode of microcrack alignment and the effective stress available for cracking. Lack of detailed information of the above factors limits the application of meso-mechanical failure models. When comparing for instance the tensile strength of the unsaturated sandstone with the unsaturated mortar (Fig. 5 and 6), it can be seen that the unsaturated mortar yields a higher tensile strength than the unsaturated sandstone. This difference in strength can be explained by a difference in any of the above mentioned factors determining the tensile strength. Which factors are responsible for the difference in tensile strength and at which measure is not clear at the moment.

The tensile strength of the closed saturated mortar specimens can be seen to be higher compared to that of the unsaturated mortar specimens (Fig. 5). This is a consequence of the closed condition in the experiments

where no fluid can penetrate the specimen during the test. In uniaxial tension, the volume of the specimen, or more precisely the pore volume, increases. This has no consequence for the unsaturated material, since the pores are filled with highly expandable air. For the saturated material, an equal expansion of the water in the enlarged pore space will lead to negative pore pressures, due to the surface tension of the water. The negative pore pressures will increase the cohesion of the material (see Fig. 7b), and thus the tensile strength.

The tensile strength of the open, water saturated sandstone specimens is lower than that of the unsaturated closed sandstone specimens (Fig. 6). For the closed unsaturated sandstone specimens, the pore pressures remain zero, for the same reasons as discussed above. For the open saturated sandstone specimens, no negative pore pressures can develop since the water from the reservoir of the cell is free to enter the specimens. Reduction in apparent tensile strength of the saturated sandstone specimens is often attributed to a loss of material cohesion upon saturation. Cohesion loss might be due to weakening of the clay which serves as matrix material in the sandstone in reaction on the presence of the water (Alonso et al., 1987).

4.2 Failure envelopes.

The tensile failure envelopes in Fig. 5 and Fig. 6 are expressed as linear functions of the axial and radial stresses at failure. In the previous section, it was argued that the ability of the global uniaxial tensile stress to cause local tensile failure depends on the magnitude of the local tensile stress. The same criterion will hold under triaxial extensile stress conditions (defined as the stress conditions for which the radial compressive stress is always larger than the axial stress). This can be understood when the radial compressive stress situation is considered first. Under both global radial compression and global uniaxial tension the dominant mode of failure is tensile failure of the bonds (compare Fig. 7a and 8a). However, local tensile failure is initiated by wedging the aggregates under radial compressive loading, while it is initiated by pull-apart of the aggregates under uniaxial loading. The effectiveness of the radial stress to cause local tensile failure due to wedging depends firstly on magnitude and direction of the local radial stresses at the contact between the aggregates. Secondly, it depends on the packing and geometry of the aggregates. For instance, local compressive contact stresses parallel to the direction of the global radial compressive stress will not cause wedging at all.

Under triaxial extensile stress conditions, the local tensile stress is a weighted contribution of axial and radial global stresses, as expressed by

the failure envelope functions. As seen in the previous section, the tensile strength does not reflect the local tensile stress, but the global uniaxial tensile stress at failure only. Hence, the failure envelope expressions give only the relative contribution of the two global failure stresses. It is due to under-determined failure expressions that failure criteria in terms of effective global axial stresses is not possible at the moment.

For the unsaturated materials, the contributions of axial and radial stress differ strongly between the two materials (see Fig.5 and 6). For the unsaturated mortar, the radial stress contributes as much to tensile failure as the axial stress, while for the unsaturated sandstone, its contribution is very low. At the moment it is not clear what causes the strong difference in radial stress contribution between the unsaturated materials.

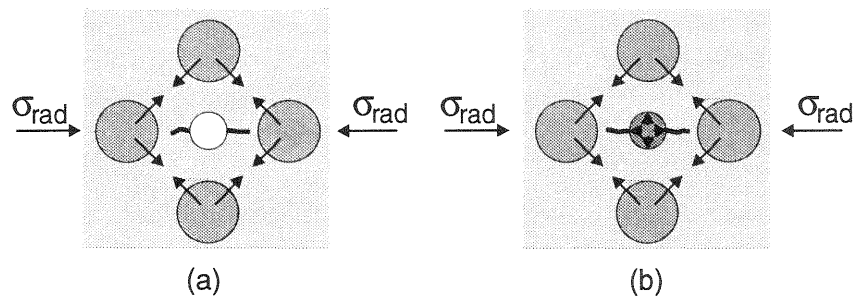


Fig. 8 Reaction forces under a global radial compressive stress for an unsaturated (a) and a saturated (b) porous material. The global radial stress is in the plane perpendicular to the drawing

For the saturated closed mortar specimen, the contribution of the radial stress is reduced in comparison to the contribution to unsaturated failure (fig. 5). This is a consequence of the pore pressures, generated by the external stresses. The hydrostatic pore pressures counteract the global radial compressive stress, hence reducing the local radial stress available to wedge the aggregates (see Fig. 8b) and thus its contribution to global tensile failure. The pore pressures have an opposite effect in the axial direction. As a result, a shift in contribution of global axial and radial stress to tensile failure will occur.

The increase in radial stress contribution for the open, saturated sandstone compared to the closed, unsaturated specimen is a consequence of the open test condition. In these experiments, the pore pressure is equal to the radial fluid pressure due to the open structure of the material. Hence, the tensile failure criterion for the saturated response curve can be

given in terms of effective axial stress: $f_t = \sigma'_{ax} = \sigma_{ax} - p_p$ and the effective radial pressure $\sigma'_{rad} = \sigma_{rad} - p_p = 0$. It thus seems that the radial compressive stress in this case does not contribute to the tensile failure at all, and an effective axial stress law suffices. Similar effective axial failure stress criteria for the other three failure curves have not been found yet. It seems that the effect of the radial stress on these failure envelopes can not be neglected.

5 Conclusions

Tensile failure of heterogeneous materials is governed by a local stress equilibrium of global stresses. The contributions of the global radial compressive stresses to tensile failure can not be neglected, since they may contribute as much to the tensile failure as the global axial stress. In addition, tensile failure of fluid saturated materials is influenced by the pore pressures. The hydrostatic pore pressures reduce the effects of the global compressive stresses and increases the effects of global tensile stresses on the material. However, they do not basically change the failure mode. A failure criterion based on an effective axial stress (global axial stress minus the effect of the pore pressures) only is not valid, except for the trivial case when the effective radial stress is zero. Other failure criteria however have not yet been tested.

References

- Alonso, E.E., Gens, A. and Hight, D.W. (1987) Special problem soils: general report, in **Proc. 9th European Conference on Soil Mechanics and Foundation Engineering**, Balkema, Rotterdam, vol.3, 1087-1146.
- Mindess, S. (1989) Interfaces in concrete, **Material Science of Concrete I**, (ed J. Skalny), American Concrete Society, 163-180.
- Visser, J.H.M. and van Mier, J.G.M. (1992) Hydraulically driven fractures of concrete and rock: a new test cell, in **Fracture Mechanics of Concrete Structures** (ed Z.P. Bazant), Elsevier Applied Science, London, 512-517.
- Visser, J.H.M. (1995) Tensile hydraulic fracturing of concrete and rock. Ph.D.-thesis (in preparation).